Assessing the impact of carbon nanotubes on the damping and parametric instability responses of glass fiber reinforced composite cylindrical shells

Mokadem, Khadra; Mattipally, Prasad; Ghori, Syed Waheedullah; Alzlfawi, Abdullah; Kumar, Alok; Al-Bahrani, Mohammed; Siddique, Mohammed Javeed; Jindal, Prakhar; Selvaraj, Rajeshkumar; Cruz, Dany Tasan

DOI
10.1016/j.jcomc.2025.100669

Publication date
2025

Document Version
Final published version

Published in
Composites Part C: Open Access

Composites Part C: Open Access 18 (2025) 100669

Contents lists available at ScienceDirect

Composites Part C: Open Access

journal homepage: www.sciencedirect.com/journal/composites-part-c-open-access

Assessing the impact of carbon nanotubes on the damping and parametric instability responses of glass fiber reinforced composite cylindrical shells

Khadra Mokadem [a], Prasad Mattipally [b], Syed Waheedullah Ghori [c], Abdullah Alzlfawi [d], Alok Kumar [e], Mohammed Al-Bahrani [f], Mohammed Javeed Siddique [g], Prakhar Jindal [h,*], Rajeshkumar Selvaraj [i,**], Dany Tasan Cruz [j]

[a] Kasdi Merbah Ouargla University, VPRS Laboratory, B.P. 511, 30000, Ouargla, Algeria
[b] Department of Physics, Hyderabad Institute of Technology and Management, Gowdavelly Village, Telangana, 501401, India
[c] Mechanical Engineering Department, College of Engineering, King Khalid University, Abha, Saudi Arabia
[d] Department of Civil and Environmental Engineering, College of Engineering, Majmaah University, Al Majmaah 11952, Saudi Arabia
[e] Mechanical Engineering Department, Nalanda College of Engineering, Chandi, Bihar Engineering University, Patna, Bihar, India
[f] Chemical Engineering and Petroleum Industries Department, Al-Mustaqbal University, Babylon, 51001, Iraq
[g] Department of Civil and Construction Engineering, A'Sharqiyah University, Ibra, Oman
[h] Space System Engineering, Faculty of Aerospace Engineering, Delft University of Technology (TU Delft), Netherlands
[i] Department of Mechanical Engineering, Arulmigu Meenakshi Amman College of Engineering, Tiruvannamalai, Tamil Nadu, India
[j] Universidad Politécnica de Madrid, Escuela Técnica Superior de Edificación, Spain

ARTICLE INFO

Keywords:
Cylindrical shell
Carbon nanotubes
Mechanical characterization
Vibration analysis
Damping characteristics
Instability behavior

ABSTRACT

This work examines the vibration, damping, and instability properties of cylindrical shells comprised of glass fiber-reinforced polymer (GFRP) composite reinforced with carbon nanotubes (CNT). The 2 wt.% CNT-reinforced composites are created using the vacuum-assisted hand layup method. An experimental investigation was done to examine the material characteristics of CNT-reinforced GFRP composites. The results indicate that the CNT reinforced composite exhibits superior material characteristics. A finite element method-based higher-order shear deformation theory (HSDT) is used to obtain the governing equations for the cylindrical shell. Further, a thorough parametric study is conducted to examine the effect CNT reinforcement, curvature ratio, thickness ratio and aspect ratio on the vibration, damping, and instability characteristics of the cylindrical GFRP shell. From the obtained results, it can be concluded that the 2 wt.% CNT reinforcement greatly influences the vibration, damping, and instability characteristics of the cylindrical shells.

1. Introduction

Fiber-reinforced composite shell structures have gained significant importance in high-performance structural applications, such as transportation, naval, and aerospace, because of their high fatigue strength, longevity, and modulus-to-weight ratio [1]. Growing use of composite structures in structural applications, including windmill, turbine, propeller, and helicopter rotor blades, has resulted in the disastrous effect of resonance in structures [2]. The upcoming generation of composites improves the structural elastic and damping properties by adding multiwall carbon nanotubes (MWCNT) as secondary reinforcement in fiber-reinforced composites [3]. The exceptional qualities of MWCNT, including exceptionally high specific strength, specific stiffness, damping, and fatigue along with excellent electrical and thermal properties, are the reason for the notable improvement in the structural performance of CNT nanocomposites [4]. Although a great deal of research has gone into developing CNT-reinforced polymer nanocomposites for a range of structural applications, it is still in its infancy because of CNT agglomeration and inadequate interfacial adhesion between CNT and resins [5]. The agglomerated and entangled nanotubes in CNT reinforced composites attenuate their mechanical properties. To overcome the difficulties in processing composite materials, researchers suggested a variety of dispersion techniques, including functionalization and physical blending [6]. The combined effects of mechanical stirring and

* Corresponding author at: Space System Engineering, Faculty of Aerospace Engineering, Delft University of Technology (TU Delft), Netherlands.
** Corresponding author at: Department of Mechanical Engineering, Arulmigu Meenakshi Amman College of Engineering, Tiruvannamalai, India.
E-mail addresses: p.jindal@tudelft.nl (P. Jindal), srajeshin1@gmail.com (R. Selvaraj).

https://doi.org/10.1016/j.jcomc.2025.100669

Available online 24 October 2025

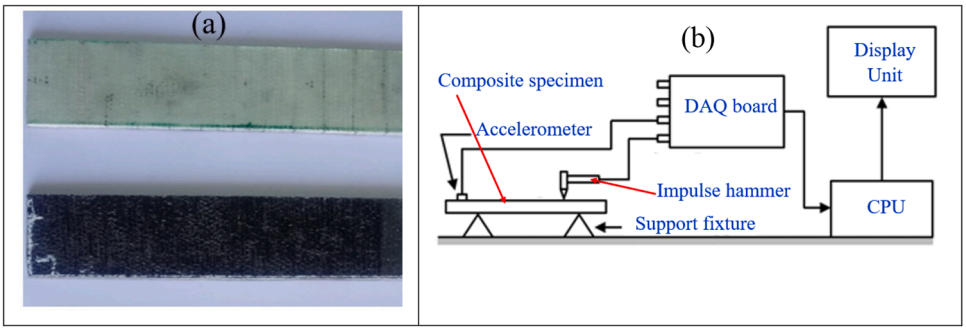

Fig. 1. (a) Specimens picture (b) photograph of test setup.

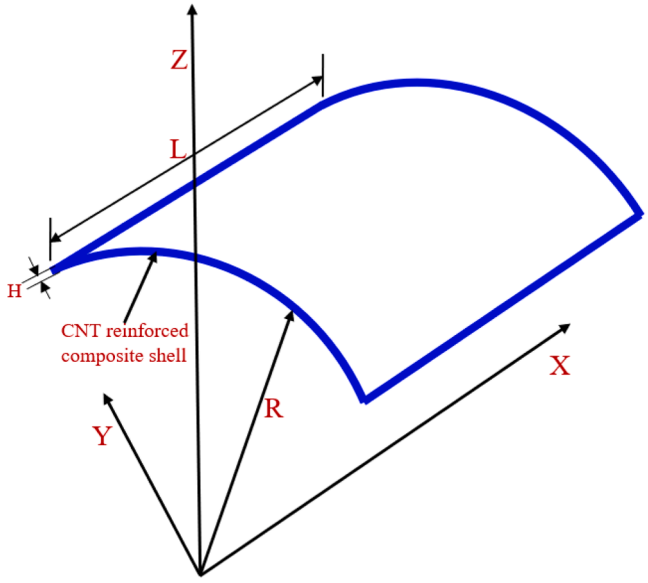

Fig. 2. Schematics of the cylindrical composite shell.

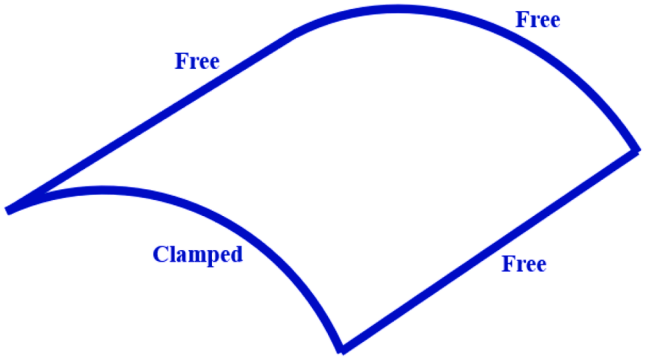

Fig. 3. Schematic representation of clamped free (CFFF) end condition.

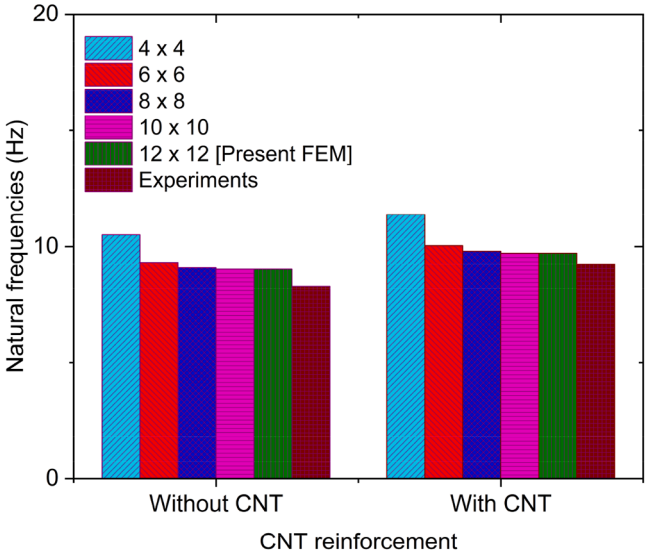

Fig. 4. Comparison of natural frequencies with FEM and experiments [41].

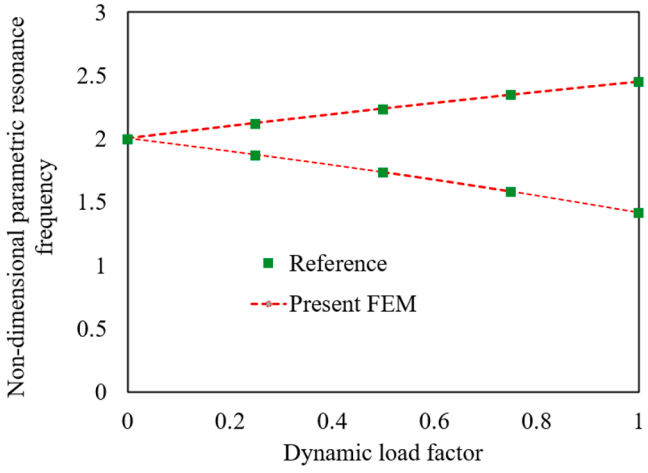

Fig. 5. Non-dimensional parametric instability region.

three roll milling techniques used for the dispersion of graphene nanoplatelets into the epoxy matrix were studied by Shadlou et al. [7]. Mechanical stirring was used for 15 min at 2000 rpm to reinforce the various weight percentages of graphene nanoplatelets particles (0.25, 0.50, and 1 wt %) to the epoxy resin matrix. Three rolls are milled at the appropriate speed and duration after the mechanical stirring process. Comparing the 1 wt percent graphene nanoplatelet reinforced epoxy composites with the neat epoxy, the results showed that the yield strength and Young's modulus increased to 20 % and 10.3 %, respectively. Prolongo et al. [8] looked into the combined impact of the three-roll milling and sonication processes used to disperse the graphene nanoplatelets into the epoxy resin matrix. The initial step involved reinforcing the various weight percentages of graphene nanoplatelets (1.50, 2.0, 3.0, 5.0, and 8.0 wt. %) to the epoxy matrix using a sonication probe for 45 min at 0.5 s, 400 W, and 50 % power and amplitude during the sonication cycle. Following the sonication process, three rolls were milled for speed, with a gap of five micrometers and 250 rpm between

Table 1
Comparison of natural frequencies (Hz) with Liao et al. [42].

Laminated shell	Mode	Liao et al. [42]	Present FEM	Deviation
Without graphene	1, 1	4.6	4.84	5.11
	1, 2	15.35	15.01	2.20
	2, 1	28.58	28.91	1.15
	2, 2	51.08	48.07	5.89
	1, 3	79.59	82.18	3.25
With graphene	1, 1	4.94	5.20	5.36
	1, 2	16.51	16.16	2.11
	2, 1	30.7	31.12	1.37
	2, 2	54.93	51.75	5.80
	1, 3	85.52	88.46	3.44

each pair. Comparing the graphene nanoplatelets incorporated epoxy-based nanocomposites sample to neat epoxy and other nanocomposites specimens, the results showed that the tensile modulus of the 3-weight percent increased to 11.4 %.

The elastic properties of functionally graded carbon nanotubes (FG-CNT) reinforced composite evaluated using the equivalent inclusion-average stress method showed close agreement, according to Aragh et al. [9]. Shen and colleagues [10] determined the CNT efficiency parameter for different volume fractions of CNT-reinforced nanocomposite by contrasting the mechanical properties determined by the extended rule of mixture with the molecular dynamic's simulations. According to Thostenson and Chou [11], adding 5 wt percent of CNTs improved the elastic modulus by 49 % in an aligned nanotube composite and 10 % in a randomly orientated composite. Pan et al. [12] used both theoretical and experimental techniques to examine the damping properties of CNT-reinforced composite beams. According to their findings, the damping ratio of the 0.4 wt percent CNT-reinforced beam is 41 % better than that of pure epoxy. Using an axisymmetric model, Behdinan et al. [13] examined the heat transfer characteristics of FG axisymmetric cylinders reinforced with graphene and carbon nanotubes. The impact of carbon nanotubes (CNT) on the elastic characteristics of a high-density polyethylene (HDPE) composite was investigated experimentally by Fattahi et al. [14]. Their findings demonstrated that the composites' Young's modulus drops as the CNT reinforcement increases above 1 wt percent. The damping characteristics of epoxy resin-based composite beams reinforced with graphene nanoplatelets (GNPs) and carbon nanotubes (CNTs) were examined by Pan et al. [15]. According to their findings, the first-order loss factor rose by 128.9 % at 0.025 wt percent GNPs in comparison to pure epoxy.

Panda et al. [16] investigated how moisture affected the natural frequencies of doubly curved GFRP panels and found that increased moisture concentrations significantly decreased frequencies. The dynamic stability of GFRP shallow shells in a hygrothermal environment was investigated by Biswal et al. [17] using first order theory. Using both numerical and experimental techniques, Patel et al. [18] examined the effects of varying CNT percentages on the natural frequencies of composite plates. Their results show that the influence of MWCNT raises the natural frequencies. Vibrations of plates, vibrations of shells, buckling of plates, and vibration/buckling in shells constructed of CNTRCs have all been studied using different methods [19–26]. The impact of hygrothermal ageing on cotton/E-glass fiber reinforced with graphene oxide was examined by Russell et al. [27]. The effects of hygrothermal ageing on an E-glass/ of interpenetrating polymer networks (IPN) composite reinforced with nanoclay were investigated by Naveen Kumar et al. [28]. The mechanical, free vibration and thermal characteristics of nanoclay and E-glass fiber-reinforced composites were investigated by

Table 2
The influence of CNT on the natural frequencies of the cylindrical shells.

CNT	End conditions	Mode (m, n)	Curvature ratio (R/L)				
			1	2	5	10	∞
0 wt. %	CFFF	1, 1	26.87	25.27	24.80	24.73	24.70
		1, 2	41.63	42.29	42.49	42.52	42.53
		2, 1	146.75	152.35	154.23	154.10	147.96
		2, 2	155.85	172.69	179.73	172.40	156.55
	CFCF	1, 1	431.43	433.26	376.14	234.15	157.01
		1, 2	625.91	502.82	381.64	241.98	168.19
		2, 1	782.32	696.55	429.32	300.52	241.08
		2, 2	793.01	703.24	433.62	433.64	433.63
	CCCC	1, 1	727.98	554.17	409.98	279.90	217.48
		1, 2	873.19	749.40	487.91	458.36	421.39
		2, 1	1114.90	799.40	552.58	477.33	473.72
		2, 2	1129.40	893.93	657.63	634.02	625.91
1 wt. %	CFFF	1, 1	27.92	26.27	25.78	25.71	25.68
		1, 2	43.24	43.93	44.14	44.17	44.18
		2, 1	152.53	158.35	160.30	160.15	153.55
		2, 2	161.94	179.44	186.75	178.96	162.71
	CFCF	1, 1	448.43	450.34	390.78	243.30	163.19
		1, 2	650.24	522.50	396.49	251.42	174.79
		2, 1	813.10	723.69	445.99	312.18	250.44
		2, 2	824.18	730.80	450.70	450.72	450.71
	CCCC	1, 1	756.25	575.85	425.94	290.80	225.94
		1, 2	907.47	778.77	507.11	475.93	437.50
		2, 1	1158.50	830.48	573.84	496.12	492.38
		2, 2	1173.20	928.74	683.28	658.76	650.34
2 wt. %	CFFF	1, 1	26.97	25.36	24.88	24.81	24.78
		1, 2	41.96	42.63	42.84	42.87	42.88
		2, 1	147.25	152.85	154.72	154.57	148.58
		2, 2	156.72	173.63	180.70	173.45	157.26
	CFCF	1, 1	432.93	434.74	377.36	234.91	157.52
		1, 2	630.31	505.47	382.97	242.89	168.92
		2, 1	785.09	701.31	431.28	302.12	242.58
		2, 2	796.07	705.65	435.08	435.09	435.09
	CCCC	1, 1	733.58	557.49	411.67	281.17	218.58
		1, 2	877.52	752.65	490.26	460.80	423.74
		2, 1	1122.50	805.03	555.28	479.51	475.84
		2, 2	1138.10	898.77	661.71	637.82	629.61

Table 3
The influence of CNT on the loss factors of the cylindrical shells.

CNT	End conditions	Mode (m, n)	Curvature ratio (R/L)				
			1	2	5	10	∞
0 wt. %	CFFF	1, 1	0.015352	0.015541	0.015602	0.015612	0.015617
		1, 2	0.012658	0.012526	0.012492	0.012488	0.012487
		2, 1	0.015534	0.015579	0.015597	0.015584	0.014711
		2, 2	0.014174	0.014216	0.014236	0.014044	0.015243
	CFCF	1, 1	0.015525	0.015541	0.015528	0.015548	0.015585
		1, 2	0.013215	0.014354	0.015382	0.015223	0.014924
		2, 1	0.015480	0.013572	0.014878	0.014520	0.014102
		2, 2	0.015272	0.015498	0.015546	0.015547	0.015547
	CCCC	1, 1	0.012951	0.014110	0.015245	0.015107	0.014920
		1, 2	0.014737	0.015108	0.014921	0.014794	0.014716
		2, 1	0.013769	0.013667	0.014908	0.015082	0.015139
		2, 2	0.013087	0.014570	0.014354	0.014516	0.014577
1 wt. %	CFFF	1, 1	0.021706	0.021886	0.021936	0.021940	0.021939
		1, 2	0.019694	0.019608	0.019589	0.019588	0.019588
		2, 1	0.021903	0.021922	0.021911	0.021853	0.021763
		2, 2	0.020862	0.020891	0.020906	0.021561	0.022082
	CFCF	1, 1	0.021883	0.021877	0.022070	0.022023	0.021908
		1, 2	0.020160	0.021006	0.021952	0.021774	0.021427
		2, 1	0.021831	0.020644	0.021738	0.021557	0.021335
		2, 2	0.021668	0.021914	0.021869	0.021865	0.021864
	CCCC	1, 1	0.020106	0.021016	0.022076	0.022080	0.022063
		1, 2	0.021408	0.021772	0.021647	0.022294	0.022361
		2, 1	0.020904	0.020986	0.022164	0.021772	0.021816
		2, 2	0.020395	0.021604	0.021646	0.021802	0.021860
2 wt. %	CFFF	1, 1	0.022979	0.023141	0.023202	0.023218	0.023228
		1, 2	0.021898	0.021864	0.021851	0.021849	0.021848
		2, 1	0.023108	0.023173	0.023219	0.023277	0.022235
		2, 2	0.022535	0.022578	0.022592	0.021510	0.022452
	CFCF	1, 1	0.023104	0.023142	0.022935	0.023018	0.023198
		1, 2	0.022126	0.022613	0.022881	0.022880	0.022884
		2, 1	0.023070	0.022005	0.022446	0.022168	0.021855
		2, 2	0.022986	0.023026	0.023161	0.023166	0.023169
	CCCC	1, 1	0.021829	0.022262	0.022522	0.022317	0.022062
		1, 2	0.022586	0.022666	0.022572	0.021581	0.021377
		2, 1	0.021898	0.021685	0.021920	0.022633	0.022655
		2, 2	0.021641	0.022145	0.021775	0.021796	0.021804

Naveen Kumar et al. [29]. The effect of interlaminar glass fiber hybridization on the static mechanical and modal properties of jute and flax composites was examined by Pingulkar et al. [30]. According to their research, hybrid composites improved modal characteristics. The mechanical and vibrational characteristics of composites composed of glass and jute fibers with different volume percentages of SS304 and aluminium wire mesh were examined by Salve and Mache et al. [31]. According to their findings, tensile strength was increased by 26 % when steel wire mesh was hybridized with jute epoxy composite.

The impact of twist, rotational speed, and tapering angles on the natural frequencies of rotating twisted composite beams is studied numerically by Rao et al. [32]. According to Deepak et al.'s [33] investigation into the impact of rotational speed on the dynamic characteristics of CNT-reinforced polymer nanocomposite beams, rotating beams with CNT reinforcement had much higher vibrational frequencies than rotating beams without CNT reinforcement. Researchers discovered that adding 2 wt percent of CNT to carbon fiber composite enhanced the damping by 130 % and 150 %, respectively, in stationary and rotating composite beams. Dai et al. [34] used the Haar wavelet discretization method and thin shell theory to study the damping properties of spinning cylindrical laminated composite shells. The study discovered that when rotating speeds increase, the damping values of shells drop and frequency rises. The influences of plate length to width ratio, skew angle, and fiber orientation on the primary and secondary instable zones of composite plates were explored by Dey and Singha [35]. Park and Lee [36] employed higher order theory to examine the impact of delamination on the parametric stability of spherical structures subjected to in-plane periodic loads. The zones of functionally graded CNT reinforced composite beam dynamic instability were studied by Ke et al. [37]. The incorporation of more CNT results in an increase in the dynamic characteristics and crippling loads of evenly dispersed and FG-CNT reinforced nanocomposites. Wang et al. [38] suggested an analytical method to examine the dynamic instability of a MWCNT reinforced nanocomposite using the Donnell-shell model. With the addition of MWCNT, the stiffness of the composite was improved, potentially leading to a considerable increase in the parametric resonance frequency under inplane loads. Fu et al. [39] looked at the dynamic stability of a laminated FG-CNT reinforced conical shell surrounded by elastic foundations. They demonstrate that the instability area grows with increasing CNT content.

It should be noted that the majority of the papers listed above have concentrated on the buckling and free vibrations of composite plates. Additionally, the damping properties of the GFRP composite cylindrical shells reinforced with CNTs have not yet been studied. According to the authors' knowledge, the vibration, damping and instability characteristics of the CNT-reinforced GFRP cylindrical shells have not been attempted. The current work includes several novel contributions that set it apart from our previous research on composite structures. First, the use of multi-walled carbon nanotubes (MWCNTs) as secondary reinforcements in GFRP shells is thoroughly investigated using both experimental and numerical methods. Second, we performed experimental studies on CNT-reinforced composites to determine the material properties. These material characteristics are then applied directly in the finite element model. This experimental-numerical linkage represents a significant improvement over our previous methodologies. Third, the numerical formulation used here is based on higher-order shear deformation theory, which captures through-thickness effects more accurately than previous publications' first-order models. The numerical results in the literature for composite shells are confirmed by using the present formulation, which results in high degree of agreement. Finally,

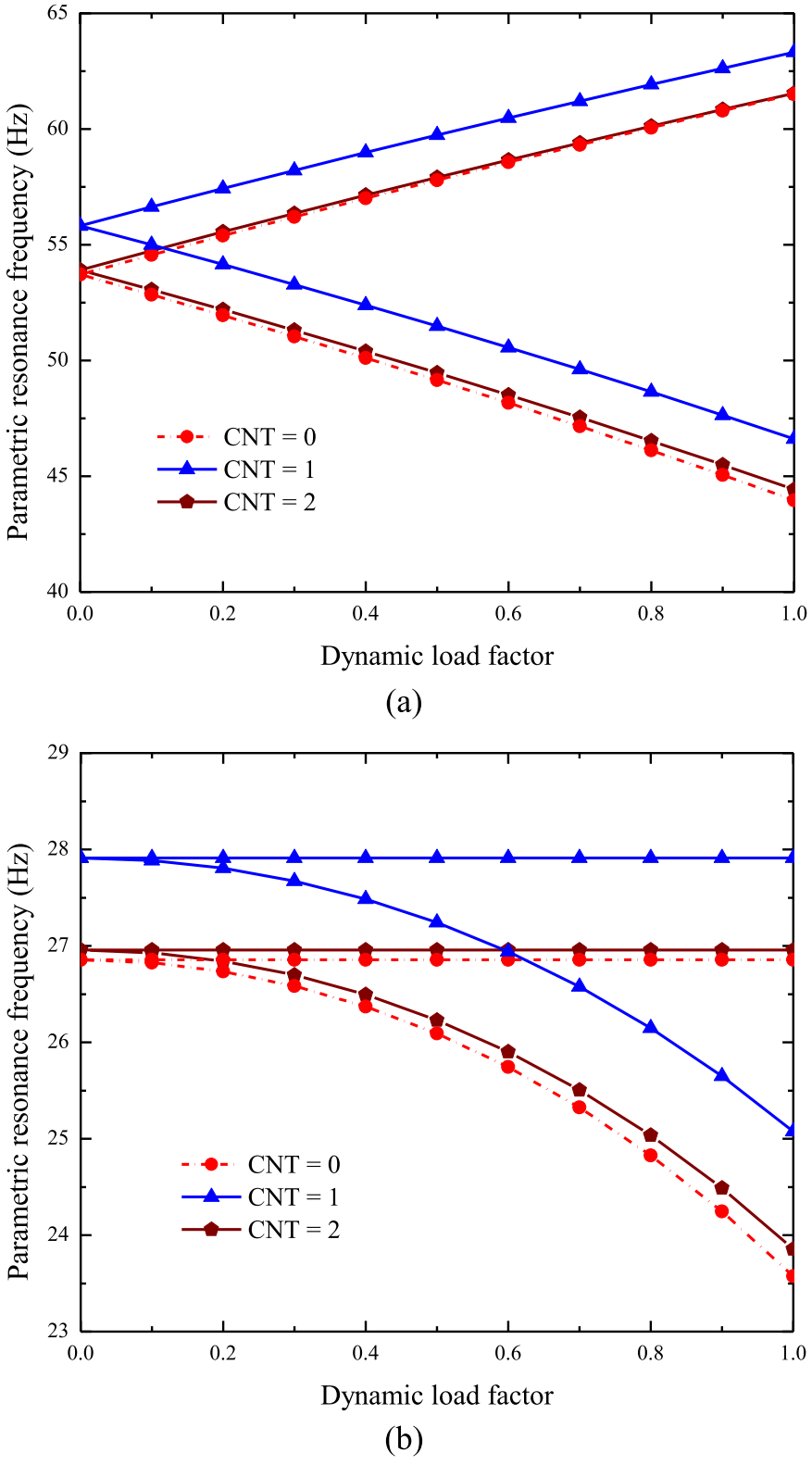

Fig. 6. (a) Principal instability regions (b) Second instability region.

the effects of various aspects, including CNT reinforcement, curvature ratio, thickness ratio and aspect ratio on the vibration, damping, and instability behavior of cylindrical shells are examined and discussed.

2. Fabrication and characterization

2.1. Fabrication of CNT reinforced composites

The raw materials used for the fabrication process are glass fiber (unidirectional 220 GSM), epoxy resin, and hardener, which were

Table 4
The influence of aspect ratio on the natural frequencies of cylindrical shells.

CNT	Curvature ratio (R/L)	Mode (m, n)	Thickness ratio			
			50	100	150	200
Without CNT	1	1, 1	47.47	24.62	17.32	13.87
		1, 2	73.97	38.06	26.34	20.67
		2, 1	257.65	134.62	95.17	76.50
		2, 2	273.35	142.81	100.05	79.50
	2	1, 1	45.55	23.03	15.61	11.97
		1, 2	76.18	38.51	25.97	19.75
		2, 1	273.53	138.87	94.20	72.22
		2, 2	309.15	157.41	106.61	81.45
	5	1, 1	44.99	22.56	15.09	11.36
		1, 2	76.87	38.65	25.85	19.44
		2, 1	278.29	140.33	93.94	70.74
		2, 2	318.4	163.54	109.49	82.42
	10	1, 1	44.91	22.48	15.01	11.26
		1, 2	76.97	38.67	25.83	19.39
		2, 1	276.02	140.25	93.81	70.47
		2, 2	289.47	159.84	109.93	82.55
	∞	1, 1	44.88	22.45	14.97	11.23
		1, 2	77.01	38.67	25.82	19.37
		2, 1	268.07	134.54	89.77	67.33
		2, 2	283.45	142.36	95.01	71.26
With CNT	1	1, 1	47.65	24.71	17.39	13.93
		1, 2	74.57	38.36	26.55	20.83
		2, 1	258.55	135.08	95.50	76.76
		2, 2	274.91	143.6	100.59	79.92
	2	1, 1	45.71	23.10	15.66	12.01
		1, 2	76.80	38.82	26.18	19.91
		2, 1	274.45	139.33	94.519	72.46
		2, 2	310.87	158.27	107.19	81.89
	5	1, 1	45.14	22.63	15.13	11.39
		1, 2	77.50	38.97	26.06	19.60
		2, 1	279.17	140.78	94.24	70.97
		2, 2	320.36	164.42	110.08	82.86
	10	1, 1	45.05	22.55	15.05	11.30
		1, 2	77.60	38.98	26.04	19.55
		2, 1	276.89	140.67	94.11	70.70
		2, 2	291.16	160.82	110.52	82.99
	∞	1, 1	45.02	22.53	15.03	11.27
		1, 2	77.64	38.99	26.03	19.53
		2, 1	269.20	135.11	90.15	67.62
		2, 2	284.77	143.01	95.44	71.58

purchased from SM Composites, Chennai, India. CNT was supplied by Bottom-Up Technologies, Bangalore, Karnataka, India. The sonication method was selected to combine CNT with epoxy resin. Initially, CNT was mixed with acetone (purchased from SM Composites, Chennai, India). After that, the mixture was subjected to an hour-long sonication (Ultrasonic liquid processor, Model: ULP750, Ultrasonic Solutions, Bengaluru, India) with a 3-second pulse on/off period. The epoxy (LY556) was maintained at 70 °C (Industrial Oven, Model: LEO – 1071, The National scientific suppliers, Pondicherry, India) for one hour during that period. The CNT acetone mixture was mixed with a matrix and again sonicated for two hours with the same sonicator operating settings. The CNT-epoxy mixture is put in the oven (Industrial Oven, Model: LEO – 1071, The National scientific suppliers, Pondicherry, India) to eliminate any leftover acetone once the sonication process is complete. It was kept in this setting until the acetone coupling agent had vanished. The hand layup methodology with the vacuum infusion approach (Vacuum pump, Model: S-325S, THE I.L.E. Co, Chennai, India) was opted for manufacturing the laminated composite structure with CNT reinforcements. The E-glass fiber was used to attain a thickness of 5 mm and the samples were fabricated with 20 layers in the same stacking sequence of 0° and 90° orientation. Based on the above-mentioned matrix preparation technique, the CNT reinforced matrix was prepared and used for the fabrication. The specimens were manufactured with 0° and 90° orientation and it is showed in Fig. 1.

2.2. Mechanical characterization

The influence of CNT in the mechanical characteristics of the hybrid composite was studied through the vibration test. According to the ASTM E1876–15 [40], the samples were fabricated with the geometrical dimensions of length 150 × width 50 × thickness 5 mm^3. The density of the composites was determined using the mass to volume ratio. The vibration test [41] was conducted to determine the Young's modulus along the longitudinal and transverse directions according to the standard. Primarily the vibration test in flexural mode, the specimen was kept at the simply supported condition at two ends in line contact at the distance of 0.24 of length. The sensor was placed at 0.24 of length (L) on the top surface of the sample on one edge, and the excitation was generated at the diagonal position on the opposite edge, and the resonant frequency at flexural mode was measured from the transverse vibration response with the assistance of Dewesoft 7.1.1 (Dewesoft software, Impulse hammer and accelerometer were purchased from Atalon, Kanchipuram, India) and the experimental setup photocopy of the laminate at flexural mode is shown in Fig. 1. The material properties of the composites was determined from the vibration test through the empirical Eq. (1–4) in relation to the fundamental frequency and geometric dimensions of the composite. The loss factor of the laminated composite structure was calculated based on the circle fit method with the assistance of Dewesoft 7.1.1® software.

$$E = 0.9465\left(\frac{mf_f^2}{b}\right)\left(\frac{L^3}{t^3}\right)T_1 \tag{1}$$

$$T_1 = 1 + \left(\frac{t}{L}\right)^2 \tag{2}$$

Where, E = Dynamic Young's modulus, Pa; m = mass of the bar, g; b = width of the bar, mm; L = Length of the bar, mm; F_f = Fundamental resonant frequency on flexural mode; T_1=Correction factor for the flexure mode.

$$G = \frac{4Lmf_t^2}{bt}R \tag{3}$$

$$R = \frac{1+\left(\frac{b}{t}\right)^2}{4-2.51\frac{t}{b}\left(1-\frac{1.991}{\frac{b}{et}^{+1}}\right)}1 + \frac{0.00851n^2b^2}{L^2} - 0.060\left(\frac{nb}{L}\right)^{\frac{3}{2}}\left(\frac{b}{t}-1\right)^2 \tag{4}$$

Where, F_t = Fundamental resonant frequency at torsional mode; n = order of the fundamental resonance frequency.

The experimentally obtained material properties of the 0, 1 and 2 wt. % CNT-reinforced composites are: E_1=*27.75*±0.15 (1 + *j*0.016) *GPa*, E_2=*6.49*±0.06 (1 + *j*0.0131) *GPa*, G_{12}=*2.57*±0.03 (1 + *j*0.0104) *GPa*, G_{23}=*2.32*±0.02 (1 + *j*0.008) *GPa*, ν_{12}=*0.272*±0.0013, ρ =*1679*±9.45 *kg/m*^{3}, E_1=*30.24*±*0.21* (1 + *j*0.0213) *GPa*, E_2=*6.93*±0.09 (1 + *j*0.0263) *GPa*, G_{12}=*2.79*±0.05 (1 + *j*0.018) *GPa*, G_{23}=*2.52*±0.02 (1 + *j*0.0103) *GPa*, ν_{12} = *0.281*±0.0012, ρ =*1691*±9.60 *kg/m*^{3} and E_1=*28.39*±*0.17* (1 + *j*0.0246) *GPa*, E_2=*6.74*±0.07 (1 + *j*0.0143) *GPa*, G_{12}=*2.68*±0.03 (1 + *j*0.021) *GPa*, G_{23}=*2.49*±0.02 (1 + *j*0.0152) *GPa*, ν_{12}=*0.280*±0.0011, ρ =*1712*±9.76 *kg/m*^{3}. The CNT reinforced laminated composite exhibits superior material characteristics. The inclusion of CNT in the composite structure results in an increase of 53 % in the damping. This increase in damping indicates a significant improvement in the composite's stiffness and ability to withstand deformation under applied loads. The addition of CNT enhances the material characteristics of the hybrid laminated composite due to the stick-slip mechanism that occurs between the fiber and the CNT/epoxy. This mechanism improves load transfer efficiency and overall structural performance, making the composite more suitable

Table 5
The influence of aspect ratio on the loss factors of cylindrical shells.

CNT	Curvature ratio (R/L)	Mode (m, n)	Thickness ratio			
			50	100	150	200
Without CNT	1	1, 1	0.015343	0.015354	0.015363	0.015373
		1, 2	0.012624	0.012667	0.012726	0.012797
		2, 1	0.015495	0.015536	0.015534	0.015527
		2, 2	0.014088	0.014187	0.014257	0.014332
	2	1, 1	0.015537	0.015541	0.015539	0.015535
		1, 2	0.012515	0.012528	0.012544	0.012567
		2, 1	0.015539	0.015582	0.015586	0.015583
		2, 2	0.014168	0.014221	0.01424	0.014262
	5	1, 1	0.015597	0.015602	0.015601	0.0156
		1, 2	0.012484	0.012492	0.012494	0.012496
		2, 1	0.015547	0.0156	0.015606	0.015607
		2, 2	0.013973	0.014238	0.014244	0.014246
	10	1, 1	0.015607	0.015612	0.015612	0.015612
		1, 2	0.01248	0.012489	0.012491	0.012491
		2, 1	0.015274	0.015595	0.015611	0.015613
		2, 2	0.014508	0.013987	0.014248	0.01425
	∞	1, 1	0.01561	0.015617	0.015618	0.015619
		1, 2	0.012478	0.012488	0.01249	0.012492
		2, 1	0.014701	0.014712	0.014715	0.014716
		2, 2	0.015198	0.015247	0.015255	0.015258
With CNT	1	1, 1	0.022998	0.022974	0.022943	0.022912
		1, 2	0.021881	0.0219	0.021911	0.021923
		2, 1	0.023108	0.023102	0.023062	0.023018
		2, 2	0.022494	0.022538	0.022546	0.022551
	2	1, 1	0.023152	0.023138	0.023121	0.023101
		1, 2	0.02185	0.021866	0.021873	0.021879
		2, 1	0.023163	0.023172	0.023157	0.023137
		2, 2	0.022544	0.02258	0.022584	0.022584
	5	1, 1	0.023207	0.023201	0.023193	0.023186
		1, 2	0.021839	0.021852	0.021857	0.02186
		2, 1	0.023235	0.023217	0.023206	0.023197
		2, 2	0.021517	0.022595	0.0226	0.022601
	10	1, 1	0.023219	0.023217	0.023212	0.023208
		1, 2	0.021837	0.02185	0.021854	0.021856
		2, 1	0.023074	0.023272	0.023242	0.023227
		2, 2	0.021617	0.021527	0.022602	0.022605
	∞	1, 1	0.023224	0.023228	0.023229	0.023229
		1, 2	0.021837	0.02185	0.021853	0.021855
		2, 1	0.022231	0.022236	0.022237	0.022238
		2, 2	0.022413	0.022455	0.022462	0.022465

for high-stress applications. Additionally, the CNT reinforcement also enhances the composite's damping characteristics.

3. Mathematical modeling for cylindrical shell

The dimensions of a composite shell are taken into consideration as follows: radius of curvature *(R)*, length *(L)*, flat width *(B)* and thickness *(H)*. Fig. 2 displays the laminated shell schematic design. Expressions for displacement fields of the laminated shell according to the HSDT is represented as

$$u = u_o + z(\psi_x) - \frac{4z^3}{3h^2}(\delta_x) \tag{5}$$

$$v = v_o + z(\psi_y) - \frac{4z^3}{3h^2}(\delta_y) \tag{6}$$

$$w = w_o \tag{7}$$

The strain energies can be given as

$$U_a = \frac{1}{2}\int_v \{\varepsilon\}\,[Q]\,\{\varepsilon\}^T dv \tag{8}$$

The laminated shells' kinetic energy can be shown as

$$T = \frac{1}{2}\int_0^L\int_0^B \left\{\begin{matrix} \frac{\partial u_o}{\partial t} \\ \frac{\partial v_o}{\partial t} \\ \frac{\partial w_o}{\partial t} \\ \frac{\partial \psi_x}{\partial t} \\ \frac{\partial \psi_y}{\partial t} \\ \frac{\partial \delta_x}{\partial t} \\ \frac{\partial \delta_y}{\partial t} \end{matrix}\right\}^T \times [I] \times \left\{\begin{matrix} \frac{\partial u_o}{\partial t} \\ \frac{\partial v_o}{\partial t} \\ \frac{\partial w_o}{\partial t} \\ \frac{\partial \psi_x}{\partial t} \\ \frac{\partial \psi_y}{\partial t} \\ \frac{\partial \delta_x}{\partial t} \\ \frac{\partial \delta_y}{\partial t} \end{matrix}\right\} dxdy \tag{9}$$

The modelling of the laminated shells is done using finite element method, which use four-noded elements with seven degrees of freedom (u_o,v_o,w_o,ψ_x,ψ_y,δ_x,δ_y) at each node. The laminated shells element stiffness matrix is constructed using the strain energy calculations, and it may be shown as

$$k_a = \int_{-b}^{b}\int_{-a}^{a} [B_a(x,y)]^T \times \begin{bmatrix} A_{ij}(x) & B_{ij}(x) & E_{ij}(x) \\ B_{ij}(x) & D_{ij}(x) & F_{ij}(x) \\ E_{ij}(x) & F_{ij}(x) & H_{ij}(x) \end{bmatrix} \times [B_a(x,y)]\, dxdy \tag{10}$$

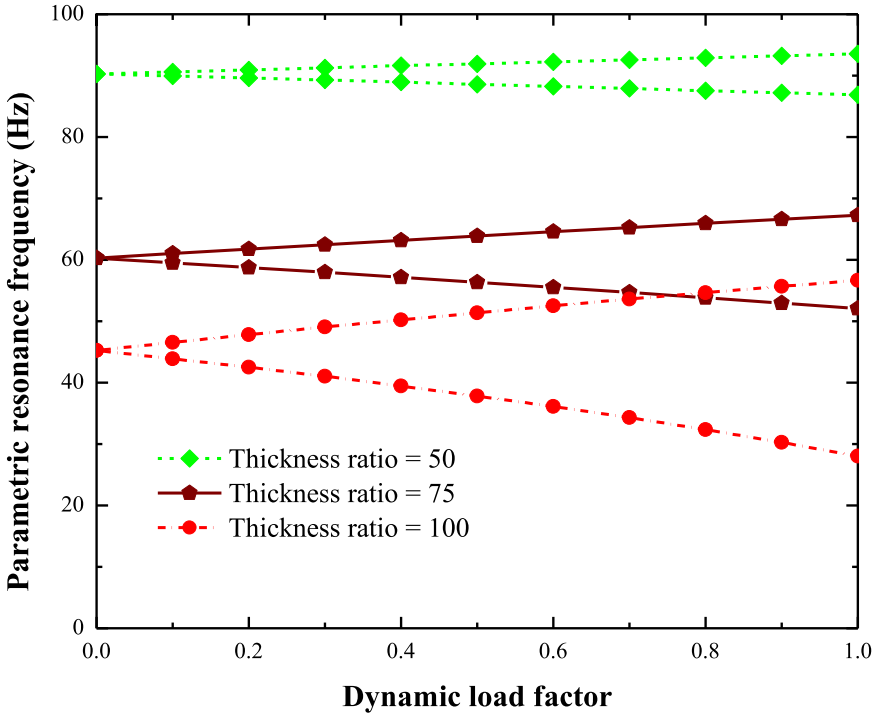

(a)

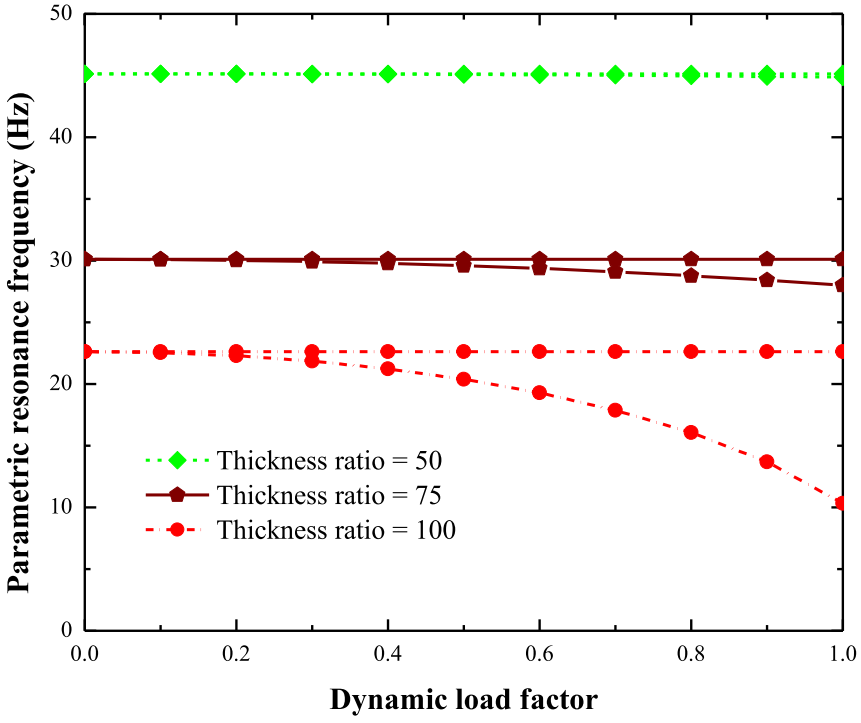

(b)

Fig. 7. (a) Principal instability regions (b) Second instability regions under different thickness ratios.

Table 6
The influence of aspect ratio on the dynamic properties of the cylindrical shells.

Aspect ratio	Mode (m, n)	Curvature ratio (R/L)			
		Natural frequencies		Loss factors	
		5	∞	5	∞
1	1, 1	24.88	24.78	0.023202	0.023228
	1, 2	42.84	42.88	0.021851	0.021848
	2, 1	154.72	148.58	0.023219	0.022235
	2, 2	180.70	157.26	0.022592	0.022452
2	1, 1	24.85	24.75	0.023247	0.023270
	1, 2	68.74	69.37	0.021504	0.021496
	2, 1	154.54	154.85	0.023260	0.023284
	2, 2	237.89	244.49	0.021925	0.021920
5	1, 1	24.80	24.71	0.023308	0.023319
	1, 2	136.34	147.57	0.021226	0.021161
	2, 1	154.31	154.72	0.023307	0.023312
	2, 2	343.75	399.71	0.021922	0.022669
10	1, 1	24.79	24.70	0.023329	0.023340
	1, 2	154.23	154.64	0.023324	0.023328
	2, 1	162.39	209.93	0.021943	0.022822
	2, 2	328.36	273.69	0.021678	0.020981

$$k_t = \int_{-b}^{b}\int_{-a}^{a} [B_t(x,y)]^T \times \begin{bmatrix} A_{ij}^s(x) & B_{ij}^s(x) & D_{ij}^s(x) & E_{ij}^s(x) \\ B_{ij}^s(x) & D_{ij}^s(x) & E_{ij}^s(x) & F_{ij}^s(x) \\ D_{ij}^s(x) & E_{ij}^s(x) & F_{ij}^s(x) & G_{ij}^s(x) \\ E_{ij}^s(x) & F_{ij}^s(x) & G_{ij}^s(x) & H_{ij}^s(x) \end{bmatrix} \times [B_t(x,y)]\, dxdy \tag{11}$$

The element mass matrix is displayed as

$$m_{ss}^e = \int_{-b}^{b}\int_{-a}^{a} [N_i(x,y)]^T [I]\, N_i(x,y)\, dxdy \tag{12}$$

The system governing equation is presented as [42]

$$[M]\left\{\ddot{d}\right\} + [K]\{d\} = \{F\} \tag{13}$$

The work done on a cylindrical shell reinforced with CNT exposed to in-plane loads may be described as

$$W_p = \frac{1}{2}\int_0^L \int_{-\frac{B}{2}}^{\frac{B}{2}} \left\{\frac{\partial w}{\partial x}\right\} P_x(t) \left\{\frac{\partial w}{\partial x}\right\} dxdy \tag{14}$$

The following governing equation describes the instability behavior of cylindrical shell

$$[M]\left\{\ddot{d}\right\} + \left([K] - \alpha\, P_{cr}\, [K_p]\right)\{d\} - (\beta\, P_{cr} \cos\omega t\, [K_P])\{d\} = \{0\} \tag{15}$$

Where $[K_P]$ is the geometric stiffness matrix.

The principal and second instability region for rotating cylindrical shells is displayed as

$$\left.\begin{aligned} &[K^*] \pm 0.5\beta P_{cr}[K_p] - 0.25\omega_1^2[M] = 0 \\ &[K^*] = [K] - \alpha P_{cr}[K_p] \end{aligned}\right\} \tag{16}$$

$$\left.\begin{aligned} &[K^*] - \omega_2^2[M] = 0 \\ &\begin{bmatrix} [K^*] & -\beta P_{cr}[K_p] \\ -0.5\beta P_{cr}[K_p] & [K^*] \end{bmatrix} - \begin{bmatrix} 0 & 0 \\ 0 & [M] \end{bmatrix}\omega_2^2 = 0 \end{aligned}\right\} \tag{17}$$

Where ω_1 and ω_2 are the principal and the second parametric resonance frequencies.

4. Results and discussion

4.1. Validation study

Fig. 3 displays the schematic representation of end condition for the curved structures with $L = 300\ mm$, $B = 50\ mm$, $R = 800\ mm$, and $H = 1.5\ mm$. The results (Fig. 4) reveal that the CNT reinforced cylindrical composite displays the greatest natural frequency, while the neat cylindrical composite has the lowest natural frequency [41]. The addition of CNT reinforcement enhances the mechanical properties of the composites, resulting in an improvement in the structural stiffness of the laminated cylindrical composite. The validation has been performed to confirm the accuracy of the HSDT model for comparison. The numerical modelling uses a mesh density of 12 × 12 since it produces better convergence results, and the corresponding findings are shown in Fig. 4. It was discovered from Fig. 4 that the numerical findings of this study were comparable to experiments [41]. Subsequently, the current model is additionally verified using available literature for the laminated composites instability regions. Fig. 5 presents the determination of the instability regions of laminated composites and a comparison with the current literature [35]. The outcomes of the current method compare favorably to the findings that have been published.

The current FE model was compared to the numerical data from Liao et al. [42]. The geometrical and material properties of the laminated shell are obtained from the reference. The comparison was carried out under cantilever end condition. It was discovered from Table 1 that the numerical findings of this study were comparable to those reported by Liao et al. [42].

4.2. Effect of CNT

The effect of CNT and curvature ratio on the dynamic analysis of the CNT-reinforced cylindrical shells is investigated. The cylindrical shell simulation is run with the following dimensions: 250 mm × 250 mm × 2.75 mm; the ply orientation is $\left[0^0/90^0/0^0/90^0/0^0/\overline{90^0}\right]_s$. The effects of CNT aggregation were incorporated by using experimentally-derived effective material properties, which inherently account for the actual CNT dispersion and clustering present in the fabricated specimens. These effective properties were directly used as input for the finite element model [43]. The dynamic analysis of the CNT-reinforced cylindrical shell is performed with the curvature ratio of 1, 2, 5, 10, and ∞ at different end conditions, and the results are presented in Tables 2 and 3. From the data, it was possible to see that the CNT reinforcement had an increase in the natural frequencies and loss factors of the cylindrical shell. The loss factor values rise by 49.68 % with the influence of CNT reinforcement. The increase in dynamic properties can be attributed to the CNTs' enhanced stiffness and damping properties. The stick-slip mechanism between the fiber and the CNT/epoxy makes the material properties of the composite better when CNT reinforcement is added. Additionally, the 2 wt. % CNT reinforced shell exhibits decreased natural frequencies and increased loss factors compared to the 1 wt. %. Due to CNT agglomeration, stiffness decreases and damping increases. We also observed a reduction in the natural frequencies of the shell as the curvature ratio increases. As expected, the flat plate's frequencies were lower than those of the shell due to the increased stiffness induced by the curvature. As expected, the flat plate's frequencies were lower than those of the shell due to the increased stiffness induced by the curvature.

The dynamic instability region (DIR) is investigated for with and without CNT-reinforced cylindrical shells. The simulated principal and secondary DIR of the cylindrical shell are displayed in Fig. 6. The principal parametric resonance frequency of the shell was found to be double its fundamental frequencies, whereas the second parametric resonance frequency is equal to the parametric resonance frequency. The parametric resonance frequencies are obtained under different dynamic load factors with a static load factor of zero. The difference

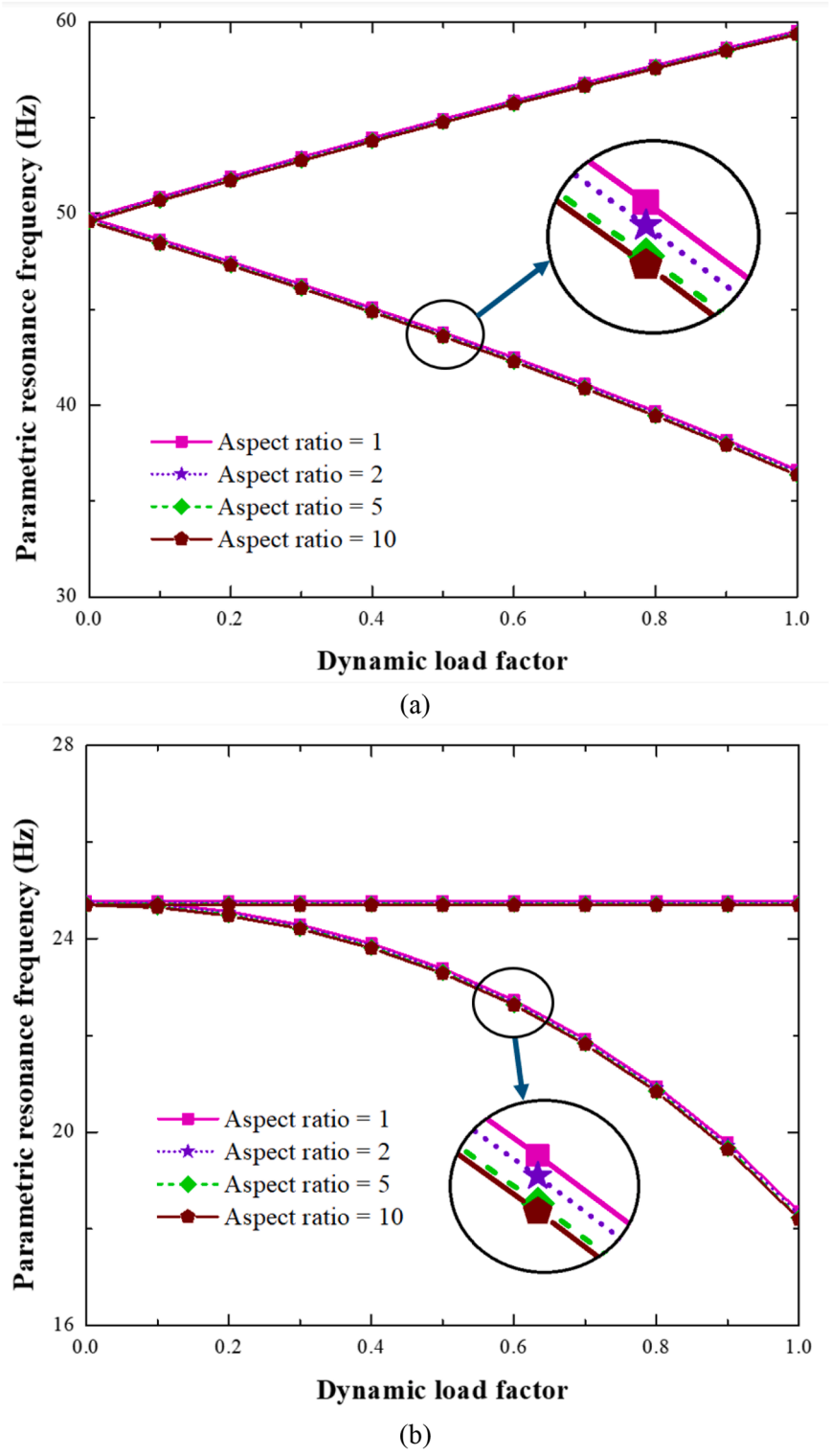

Fig. 8. (a) Principal instability regions (b) Second instability region under different aspect ratios.

between the lower and the higher parametric resonance frequency is known as the width of parametric frequency. It can be noticed that the effect of CNT reinforcement on the cylindrical shell causes the instability region to shift upward. This indicates that the random orientation of the CNTs in the composite may greatly enhance the mechanical properties of the composites, which in turn affects the cylindrical shell's instability regions. The addition of CNT reinforcement raises the shell's parametric resonance frequencies, as evidenced by this shift in the instability area. According to this shift in frequency, the addition of CNTs improves the stability and structural integrity of the shell. Additionally, it was noted that as the dynamic load increased, the width of the principal instability region increased more than the width of the second instability regions. Further, it can be inferred that the CNT-reinforced cylindrical shell significantly influences the DIR more than that of the non-CNT-reinforced shell.

4.3. Effect of thickness ratio

The dynamic responses of the CNT-reinforced cylindrical shells are examined and shown in Table 4. It can be seen that the frequency and damping values significantly influenced with an increase in the thickness ratio. According to the numerical data, the frequency values decrease by 48.14 % when the thickness ratio increases from 50 to 100. This may be explained by the fact that the stiffness of the shell grows with thickness because the stiffness of the shell is more pronounced than the mass. From Table 5, it can be noticed that the loss factor values increase with increasing the thickness ratio. This is consistent with earlier research that found a relationship between the values of the loss factor and the thickness ratio. Overall, the outcomes show that the stiffness and damping of the 2 wt.% CNT-reinforced shells are influenced by changing the thickness ratio. The dynamic instability region of the shell reinforced with CNT under periodic stress has been studied at different thickness ratio. Fig. 7 shows the DIR of the shells reinforced with CNT at different thickness ratio. The regions of instability were seen to move downward as thickness ratio increased. This is because as thickness ratio increases, so does the structural stiffness. Moreover, the dynamic instability regions of the CNT-reinforced shells are shown to be considerably influenced by the thickness ratios.

4.4. Effect of aspect ratio

Table 6 shows the impact of the aspect ratio on the vibration and damping analysis of the 2 wt.% CNT-reinforced cylindrical shell. The numerical data indicates a decrease in the fundamental mode frequency and damping, and an increase in the higher mode frequency and damping as the aspect ratio increases. This pattern is explained by the structure's increasing stiffness and decreasing mass as the aspect ratio rises, which alters the damping characteristics and natural frequencies. The DIR of the shells has been studied at different aspect ratios. Fig. 8 shows the DIR of the shells at different aspect ratios. The regions of instability were seen to move downward as aspect ratios increased. This occurs because the transverse dimension becomes significantly smaller than the longitudinal dimension as the aspect ratio increases. Thereby, lowering the shells' aspect ratio might produce a more stable structure when subjected to periodic loads.

5. Conclusions

This study examines the vibration, damping, and instability properties of cylindrical shells reinforced with CNT. The material properties of CNT-reinforced GFRP composites were investigated experimentally. The outcomes show that the CNT-reinforced composite has better material properties. We study the loss factors and associated frequencies of the cylindrical shells at different aspect ratio, thickness ratio and curvature ratios. It was demonstrated that the CNT reinforcement had an increase in the natural frequencies and loss factors of the cylindrical shell. The loss factor values rise by 49.68 % with the influence of CNT reinforcement. Additionally, it was shown that the effect of CNT reinforcement on the cylindrical shell causes the instability region to shift upward. It was found that when thickness ratio increased from 50 to 100, the natural frequencies of the shells decreased by 48.14 %. The regions of instability were seen to move downward as thickness ratios increased. It was noticed that as the curvature ratio increases, the frequency value decreases and the loss factor increases. It was also noted that when the aspect ratio rises, the instability regions move downward. Thus, it is feasible to conclude that the CNT reinforcement on the composites has a significant impact on the stiffness, damping, and instability regions of the cylindrical shells.

Funding

The current work was assisted financially to the Dean of Science Research at King Khalid University via the Research Groups Program under grant number RGP2/221/46.

CRediT authorship contribution statement

Khadra Mokadem: Conceptualization. **Prasad Mattipally:** Investigation. **Syed Waheedullah Ghori:** Software. **Abdullah Alzlfawi:** Software. **Alok Kumar:** Resources. **Mohammed Al-Bahrani:** Formal analysis. **Mohammed Javeed Siddique:** Validation. **Prakhar Jindal:** Data curation. **Rajeshkumar Selvaraj:** Writing – original draft. **Dany Tasan Cruz:** Visualization.

Declaration of competing interest

The authors declare that they have no known competing financial interests or personal relationships that could have appeared to influence the work reported in this paper.

Acknowledgments

The authors extend their appreciation to the Deanship of Scientific Research at King Khalid University, Saudi Arabia for funding this work through the Research Groups Program under grant number: RGP2/221/46.

Data availability

Data will be made available on request.

References

[1] R.F. Gibson, A review of recent research on mechanics of multifunctional composite materials and structures, Compos. Struct. 92 (12) (2010 Nov 1) 2793–2810.
[2] W. Zhang, T. Liu, A. Xi, Y.N. Wang, Resonant responses and chaotic dynamics of composite laminated circular cylindrical shell with membranes, J. Sound Vib. 423 (2018 Jun 9) 65–99.
[3] K.M. Liew, Z. Pan, L.W. Zhang, The recent progress of functionally graded CNT reinforced composites and structures, Sci. China Phys. Mech. Astron. 63 (3) (2020 Mar) 234601.
[4] Y. Kiani, M. Mirzaei, Rectangular and skew shear buckling of FG-CNT reinforced composite skew plates using Ritz method, Aerosp. Sci. Technol. 77 (2018 Jun 1) 388–398.
[5] X.L. Xie, Y.W. Mai, X.P. Zhou, Dispersion and alignment of carbon nanotubes in polymer matrix: a review, Mater. Sci. Eng. 49 (4) (2005 May 19) 89–112.
[6] Y. Geng, M.Y. Liu, J. Li, X.M. Shi, J.K. Kim, Effects of surfactant treatment on mechanical and electrical properties of CNT/epoxy nanocomposites, Compos. A 39 (12) (2008 Dec 1) 1876–1883.
[7] S. Shadlou, B. Ahmadi-Moghadam, F. Taheri, The effect of strain-rate on the tensile and compressive behavior of graphene reinforced epoxy/nanocomposites, Mater. Des. 59 (2014 Jul 1) 439–447.
[8] S.G. Prolongo, R. Moriche, A. Jiménez-Suárez, M. Sánchez, A. Ureña, Advantages and disadvantages of the addition of graphene nanoplatelets to epoxy resins, Eur. Polym. J. 61 (2014 Dec 1) 206–214.
[9] B.S. Aragh, A.N. Barati, H. Hedayati, Eshelby–Mori–Tanaka approach for vibrational behavior of continuously graded carbon nanotube-reinforced cylindrical panels, Compos. B 43 (4) (2012 Jun 1) 1943–1954.
[10] H.S. Shen, Nonlinear bending of functionally graded carbon nanotube-reinforced composite plates in thermal environments, Compos. Struct. 91 (1) (2009 Nov 1) 9–19.
[11] E.T. Thostenson, T.W. Chou, Aligned multi-walled carbon nanotube-reinforced composites: processing and mechanical characterization, J. Phys. D 35 (16) (2002 Aug 6) L77.
[12] S. Pan, Q. Dai, B. Safaei, Z. Qin, F. Chu, Damping characteristics of carbon nanotube reinforced epoxy nanocomposite beams, Thin-Walled Struct. 166 (2021 Sep 1) 108127.
[13] K. Behdinan, R. Moradi-Dastjerdi, B. Safaei, Z. Qin, F. Chu, D. Hui, Graphene and CNT impact on heat transfer response of nanocomposite cylinders, Nanotechnol. Rev. 9 (1) (2020 Feb 18) 41–52.
[14] A.M. Fattahi, B. Safaei, Z. Qin, F. Chu, Experimental studies on elastic properties of high density polyethylene-multi walled carbon nanotube nanocomposites. Steel and Composite structures, Int. J. 38 (2) (2021 Jan) 177–187.
[15] S. Pan, J. Feng, B. Safaei, Z. Qin, F. Chu, D. Hui, A comparative experimental study on damping properties of epoxy nanocomposite beams reinforced with carbon nanotubes and graphene nanoplatelets, Nanotechnol. Rev. 11 (1) (2022 Apr 19) 1658–1669.

[16] H.S. Panda, S.K. Sahu, P.K. Parhi, Effects of moisture on the frequencies of vibration of woven fibre composite doubly curved panels with strip delaminations, Thin-Walled Struct. 78 (2014 May 1) 79–86.
[17] M. Biswal, S.K. Sahu, A.V. Asha, Dynamic stability of woven fiber laminated composite shallow shells in hygrothermal environment, Int. J. Struct. Stab. Dyn. 17 (08) (2017 Oct 4) 1750084.
[18] A. Patel, R. Das, S.K. Sahu, Experimental and numerical study on free vibration of multiwall carbon nanotube reinforced composite plates, Int. J. Struct. Stab. Dyn. 20 (12) (2020 Nov 26) 2050129.
[19] M. Ahmadi, R. Ansari, H. Rouhi, Vibration of viscoelastic carbon nanotube reinforced composite plates, Sci. Eng. Compos. Mater. 26 (1) (2019) 70–76.
[20] R. Gholami, R. Ansari, Y. Gholami, Dynamic behavior of carbon nanotube-reinforced composite shells with different boundary conditions, Compos. Struct. 174 (2017) 45–58.
[21] A.K. Baltacıoğlu, Ö. Civalek, Vibration and buckling of laminated composite cylindrical shells using a numerical approach, Compos. Struct. 202 (2018) 374–388.
[22] H. Bisheh, Free and forced vibration analysis of composite cylindrical shells under thermal environments, Structures 51 (2023) 1622–1644.
[23] C.P. Wu, S.K. Chang, Dynamic response of laminated composite cylindrical shells under impact loading, Compos. Struct. 111 (2014) 587–601.
[24] R. Ansari, J. Torabi, R. Hassani, Buckling and vibration analysis of FG-CNT reinforced composite shells using a refined shear deformation theory, Comput. Math. Appl. 75 (2018) 486–502.
[25] Y. Sitli, O. Elmhaia, S. Mesmoudi, O. Askour, M. Rammane, Y. Hilali, O. Bourihane, Vibration and buckling analysis of FG-CNT reinforced composite cylindrical shells using finite element method, Comput. Struct. 303 (2024) 107492.
[26] P.T. Thang, Free vibration analysis of laminated composite cylindrical shells using first-order shear deformation theory, Proc. Inst. Mech. Eng. C 233 (2019) 702–712.
[27] E. Russel, B. Nagappan, P. Karsh, S. Madhu, Y. Devarajan, G. Suresh, R. Vezhavendhan, Effect of hygrothermal aging on novel hybrid composites: transforming textile waste into a valuable product, Polym. Compos. 45 (4) (2024 Mar 10) 3520–3535.
[28] M. Naveen Kumar, K.R. Vijaya Kumar, G. Suresh, M. Chinnathambi Muthukaruppan, R. Vezhavendhan, P. Chandramohan, G. Rathinasabapathi, An inclusive study on hygrothermal aging effects on tribological and physical properties of E-glass fiber reinforced interpenetrating polymer networks (IPNs) composites, Polym. Compos. (2024).
[29] M. Naveen Kumar, K.R. Vijaya Kumar, G. Suresh, M. Chinnathambi Muthukaruppan, R. Vezhavendhan, P. Chandramohan, G. Rathinasabapathi, A study on: impact on novel clay dispersion on mechanical, thermal and vibration properties of glass fiber-reinforced interpenetrating polymer networks (IPNs) hybrid composites, Polym. Compos. 45 (18) (2024 Dec 20) 16882–16897.
[30] H. Pingulkar, A. Mache, Y. Munde, I. Siva, Synergy of interlaminar glass fiber hybridization on mechanical and dynamic characteristics of jute and flax fabric reinforced epoxy composites, J. Nat. Fibers 19 (11) (2022 Nov 2) 4310–4325.
[31] A. Salve, A. Mache, Experimental study on the effects of SS304 and Aluminium reinforcements on mechanical and vibration properties in jute-epoxy composites, Polym. Compos. 45 (14) (2024 Oct 10) 13359–13377.
[32] S.S. Rao, R.S. Gupta, Finite element vibration analysis of rotating Timoshenko beams, J. Sound Vib. 242 (1) (2001 Apr 19) 103–124.
[33] B.P. Deepak, R. Ganguli, S. Gopalakrishnan, Dynamics of rotating composite beams: a comparative study between CNT reinforced polymer composite beams and laminated composite beams using spectral finite elements, Int. J. Mech. Sci. 64 (1) (2012 Nov 1) 110–126.
[34] Q. Dai, Z. Qin, F. Chu, Parametric study of damping characteristics of rotating laminated composite cylindrical shells using Haar wavelets, Thin-Walled Struct. 161 (2021 Apr 1) 107500.
[35] P. Dey, M.K. Singha, Dynamic stability analysis of composite skew plates subjected to periodic in-plane load, Thin-Walled Struct. 44 (9) (2006 Sep 1) 937–942.
[36] T. Park, Lee SY, Parametric instability of delaminated composite spherical shells subjected to in-plane pulsating forces, Compos. Struct. 91 (2) (2009 Nov 1) 196–204.
[37] L.L. Ke, J. Yang, S. Kitipornchai, Dynamic stability of functionally graded carbon nanotube-reinforced composite beams, Mech. Adv. Mater. Struct. 20 (1) (2013 Jan 1) 28–37.
[38] X. Wang, W.D. Yang, S. Yang, Dynamic stability of carbon nanotubes reinforced composites, Appl. Math. Model. 38 (11–12) (2014 Jun 1) 2934–2945.
[39] T. Fu, X. Wu, Z. Xiao, Z. Chen, Dynamic instability analysis of FG-CNTRC laminated conical shells surrounded by elastic foundations within FSDT, Eur. J. Mech.-A/Solids 85 (2021 Jan 1) 104139.
[40] ASTM E1876-15, Standard Test Method For Dynamic Young's Modulus, Shear Modulus, and Poisson's Ratio By Impulse Excitation of Vibration, ASTM International, United States, 2015, pp. 1–17.
[41] Shankar A.N., Murali Krishna S.M., Chebolu R.K., Ajay K.S. Singholi, Singh R., Rajeshkumar S., Effect of carbon nanotubes reinforcement on eigenmodes of multi-smart core sandwich composite cylindrical shell panels, Polymer Composites, 2022; 43, (2):1078-89.
[42] X. Liao, A. Manapaya, M. George, R. Selvaraj, Characterization of material, mechanical, static bending and vibration properties of glass fiber composite panels reinforced with graphene nanofillers, J. Manuf. Process. 99 (2023 Aug 4) 392–404.
[43] M. Subramani, M. Ramamoorthy, A.B. Arumugam, R. Selvaraj, Free and forced vibration characteristics of CNT reinforced composite spherical sandwich shell panels with MR elastomer core, Intern. J. Structure Stab. Dyn. 21 (10) (2021) 2150136.